Sliding Mode Control Based on Genetic Algorithm for WSCC Systems Include of SVC

E. Köse[1], K. Abacı[1], H. Kızmaz[2], S. Aksoy[2], M. A. Yalçın[2]

[1]*Department of Electronics and Computer Education, Mersin University,*
33480, Tarsus, Mersin, Turkey, phone: +903246274804
[2]*Department of Electrical-Electronics Engineering, Sakarya University,*
54080, Adapazarı, Sakarya, Turkey, phone: +902642955454
ekose@mersin.edu.tr

Abstract—In this study, in order to control the voltage of the Western System Coordinating Council (WSCC) system, a sliding mode control has been used. First, the active and reactive power values, voltage and angle values of the load-buses have been calculated. The load-buses which their voltage levels are lower than 1 pu has been identified. After that, by considering one of these load-buses, the system is transformed to the system with two load-buses and the sliding mode control model has been obtained. The sliding mode parameters have been obtained by using genetic algorithm (GA) optimization technique. From the results of simulations of this model, it is shown that the voltage of the load-buses reaches at 1 pu with a very low error.

Index Terms—Genetic algorithms, optimization, sliding mode control, static var compensator.

I. INTRODUCTION

In recent years, as industrialization rising in the world, the electric power consumption has risen. This rising revealed the problems of voltage stabilization and voltage collapse. In 2003 in New York, London, Denmark and Sweden, Italy and in 2005 in Java-Bali, Brazil and Paraguay voltage collapse problems have occurred [1], [2]. In order to solve those problems, either new electric production facilities have to be established or the existing facilities have to be used at the bounds. Due to the fact that establishing of the new facilities needs high funds, the usage of the new facilities at the bounds of their power can't be avoided.

Flexible AC Transmission Systems (SVC, etc.) devices improve the power system transmission and distribution performance. A rapidly operating Static Var Compensator (SVC) can continuously provide the reactive power required to control dynamic voltage swings under various systems conditions.

In order to get the performance of SVC devices increased, various control techniques are used. Some of these controllers are Neuro-Fuzzy Static Var Compensator [3], fuzzy-PID controller [4], adaptive controller [5], intelligent controller [6], fuzzy logic controller [7], and non-linear robust controller [8] respectively.

SVC-included electricity systems can be modelled

nonlinear. The sliding mode control technique can be used in order to control these systems. The sliding mode control parameters should be chosen optimally so that satisfies an optimal solution for efficiency. To provide the optimization, many techniques such as Genetic Algorithm (GA), Particle Swarm Optimization (PSO) and Bear Colony can be used.

In recent years GA, PSO and other computing techniques have emerged as capable of finding the optimum solution of a problem. Genetic algorithms start with a diverse set (population) of potential solutions. This allows for the exploration of many optimal points in parallel, lowering the probability of getting trapped at a local optimum. Genetic algorithms are simple to implement and are capable of locating the global optimal solution [9].

In this paper, Western System Coordinating Council (WSCC) system has been separated as two separate load-bus by using the results of the power process of the WSCC system and the system has been controlled by sliding mode control. The selected load-buses are references and include lower than 1 pu. The simulation results are given in graphs. The simulation results showed that GASMC method performs better results than SMC method in terms of accuracy.

II. GENETIC ALGORITHMS

Genetic algorithms use biological evolution to develop a series of search space points toward an optimal solution. There are five components that are required to implement a genetic algorithm: representation, initialization, evaluation function, genetic operators, and genetic parameters.

Genetic algorithms are derived from a study of biological systems. In biological systems evolution takes place on organic components used to encode the structure of living beings. These organic components are known as chromosomes. A group of chromosomes is called a population. The number of chromosomes in a population is usually selected to be between 30 and 300. Each chromosome is a string of binary codes (genes) and may contain substrings [9].

Genetic operators are the stochastic transition rules applied to each chromosome during each generation procedure to generate a new improved population from an old one. A genetic algorithm usually consists of

reproduction, crossover, and mutation operators.

Reproduction is a probabilistic process for selecting two parent strings from the population of the strings on the basis of roulette-wheel mechanism, using their fitness values. This process is accomplished by calculating the fitness function for each chromosome in the population and normalizing their values [9].

Crossover is the process of selecting a random position in the string and swapping the characters either left or right of this point with another similarly partitioned string. This random position is called the crossover point. The probability of crossover occurring for the parent chromosomes is usually set to a large value in range of 0.7 to 1.0.

Mutation is the process of random modification of string position by changing "0" to "1" or vice versa, with a small probability. It prevents complete loss of genetic material through reproduction and crossover by ensuring that the probability of searching any region in the problem space is never zero. The probability of mutation is usally assumed to be small (e.g., between 0.01 and 0.1) [9].
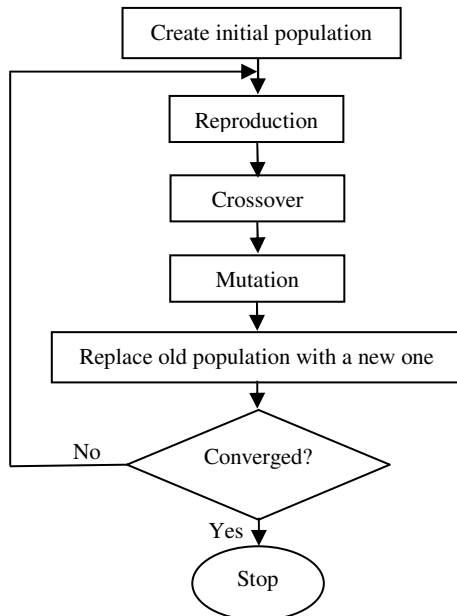

Fig. 1. Simplified flowchart of a typical genetic algorithm structure [9].

Fig. 1 shows a simplified flow-chart of an iterative genetic algorithm for optimal placement. This process is repeated until the algorithm has converged [9].

A genetic algorithm has been used in this study in order to adjust optimal sliding mode parameters used in the control input, λ, ρ and K. The block diagram of the sliding mode control system is shown in Fig. 2. Before implementing the genetic algorithm to the sliding mode control system, the cost function should be obtained. The cost function is as below

$$J(\lambda,\rho,K) = \sum_{k=0}^{\infty} [e(k)]^2 = \sum_{k=0}^{\infty} [r(k)-y(k)]^2 . \qquad (1)$$

In the search space, where the cost function is minimum, the SMC parameters will be optimum. Then, at this point, the parameters will have been found [10], [11].
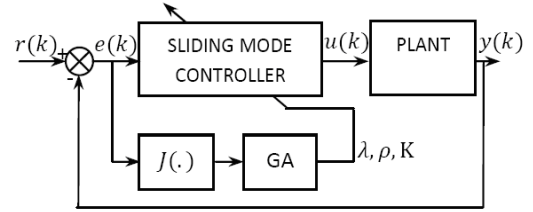

Fig. 2. SMC parameter optimization diagram.

The parameters of GA are: Population size is 50, genetic evolutional generation is 200, crossover function is scattered and mutation function is Gaussian. The parameters have been obtained as λ=34, ρ=12 and K=61 by using these GA parameters.

III. RADIAL DISTRIBUTION SYSTEMS

An interconnected power system is made up of 3 types of buses:
1) Slack bus;
2) Generator bus;
3) Load bus.

In the power system each bus is associated with four parameters such as bus voltage magnitude (V), phase angle (δ), real power (P) and reactive power (Q) [2].

In AC power systems, power flow analysis is vitally important in the planning and operation stages [12]. The various techniques proposed in the literature for power flow are such as the Newton-Raphson, the Gauss-Seidel method [12].

The power (load) flow problem consists of calculations of power flows (real, reactive) and voltages (magnitude, phase) of a network for specified (demand and generation powers) terminal or bus conditions [9].

Power system with N-load-buses which includes SVC can be separated in two load buses. The state equations of the reduced power system with two load-buses can be written as follows [13], [14]:

$$\begin{cases} \dot{\delta}(t) = \omega(t), \\ \dot{\omega}(t) = \frac{1}{M}(P_m - V_1V_2(c_1\cos\delta + c_2\sin\delta) + \frac{V_1^2(d_1b_1+d_2b_2)}{b_1^2+b_2^2} - \\ \qquad -\frac{V_1V_2}{b_1^2+b_2^2}[(d_1b_1+d_2b_2)(a_1\cos\delta + a_2\sin\delta) + \\ \qquad +(d_1b_2-d_2b_1)(a_2\cos\delta - a_1\sin\delta)] - 0.0125\omega), \\ \dot{V}_2 = \frac{1}{\tau}[(\frac{V_1V_2(b_2\cos\delta - b_1\sin\delta) - V_2^2(a_1b_2-a_2b_1)}{b_1^2+b_2^2} - \\ \qquad -V_2^2 B_{SVC} - 0.5], \\ \dot{B}_{svc} = \frac{1}{\tau}(-Vref - V_2). \end{cases} \qquad (2)$$

where $\dot{A}$=a1+ja2, $\dot{B}$= b1+jb2, $\dot{C}$= c1+jc2, $\dot{D}$= d1+jd2 and A, B, C, D are the coefficients of the π equivalent circuit of the reduced system with two gates.

IV. WESTERN SYSTEM COORDINATING COUNCIL SYSTEMS
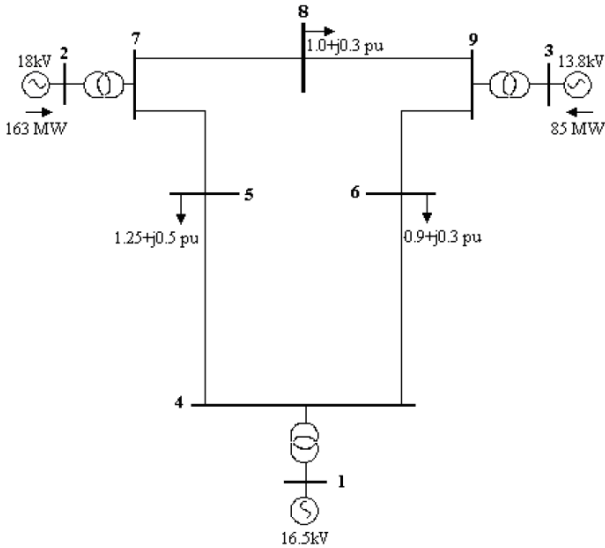
The WSCC three-machine nine-bus system is given in Fig. 3.

Fig. 3. WSCC three-machine nine-bus test systems.

Here, the base values of the system was considered as S_{base}=100MVA and V_{base}=230 kV. The powers which are consumed from the load-buses have been given as normalized pu.

The line data which belong to the transmission line of the power system with 9 buses are given in Table I, the bus voltage related to power process and angle values are given in Table II.

TABLE I. LINE DATA OF THE 9-BUS WSCC RADIAL DISTRIBUTION SYSTEM [13], [14].

Line From-To bus	R_{line}(pu)	X_{line}(pu)	Shunt admittance Y/2(pu)
4-5	0.0100	0.0850	0.1760
4-6	0.0170	0.0920	0.1580
6-9	0.0390	0.1700	0.3580
7-8	0.0085	0.0720	0.1490
5-7	0.0320	0.1610	0.3060
8-9	0.0119	0.1008	0.0522

TABLE II. POWER FLOW FOR 9-BUS WSCC RADIAL DISTRIBUTION SYSTEM NOT USED SVC [13], [14].

Bus	Bus Type	$|V|$		Active and Reactive Power	
		(pu)	δ (deg.)	P(MW)	Q(MVar)
1	Slack	1.0400	0.00	71.641	27.045
2	PV	1.0250	9.280	163.00	6.6536
3	PV	1.0250	4.664	85.00	-10.8597
4	PQ	1.0258	-2.216	0.00	0.00
5	PQ	0.9956	-3.998	-126.01	-50.44
6	PQ	1.0127	-3.6875	-87.76	-29.25
7	PQ	1.0258	3.7197	0.00	0.00
8	PQ	1.0159	0.7275	-96.9	-33.91
9	PQ	1.0324	1.9667	0.00	0.00

From the tables above, due to the fact that the voltage of the load-bus which is numbered as 5 is lower than 1 pu, this load-bus has been chosen as critical load-bus. In order to get the voltage of the load-bus numbered as 5 increased to 1 pu, the 4.8 MVar SVC has been added to load-bus numbered as 5 [13], [14].

Besides, the system has been transformed to the power system with two load-buses which was made from the load-buses numbered as 1 and 5 by using bus reducing technique. In this case, in order to get the voltage of the number 5 load-

bus increased to 1 pu, the required Y_{bus} admittance has been obtained as follows [13], [14].

$$Y_{bus} = \begin{bmatrix} 0.6649 - j7.5136 & -0.5304 + j7.5640 \\ -0.5304 + j7.5640 & -0.1526 - j7.3574 \end{bmatrix} .. \quad (3)$$

Hence, the π equivalent parameters of the system with two gates have been obtained as: $\dot{A}$ = 0.9665 - j.0879; $\dot{B}$ = 0.0092 + j0.1316, $\dot{C}$ = -0.5486 + j0.2436, $\dot{D}$ = 0.9946 + + j0.0182

The state equations of the WSCC system with the 9 load-buses has been obtained by replacing the obtained data in the equation numbered as (2). Let's design the required GASMC controller in order to the SVC system control, by using the data which are given above for the WSCC system with 9 load-bus.

V. SLIDING MODE CONTROL

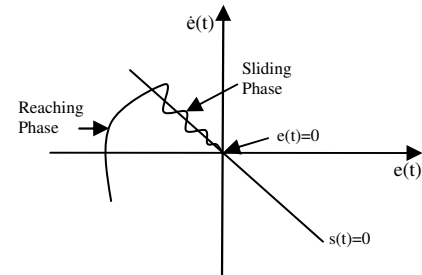SMC reaching and sliding modes consist of two phases in show Fig. 4.

Fig. 4. Phase of sliding mode control.

The nonlinear system is considered in the following canonical dynamic equations

$$x^{(n)} = f(x) + b(x)u(t) + d(t). \quad (4)$$

In this equation, $f(x)$ and $b(x)$ are uncertain nonlinear functions with known uncertainty bounds. Furthermore, the $d(t)$ function relates to the disturbance entering the system.

By assigning the desired state vector $x_d(t)$, the error state vector can be shown as follows

$$\tilde{x} = x(t) - x_d(t). \quad (5)$$

Sliding surface, which is called the switching function, is considered as follows

$$s(t) = (\lambda + \frac{d}{dt})^{(n-1)} \tilde{x}(t), \quad (6)$$

where n is the order of the uncontrolled system and λ is a positive coefficient in the real numbers set [15].

Control law always consists of two parts, the equivalent control $u_{eq}(t)$ and switching control $u_{sw}(t)$, shown in these equation:

$$u(t) = u_{eq}(t) + u_{sw}(t), \quad (7)$$
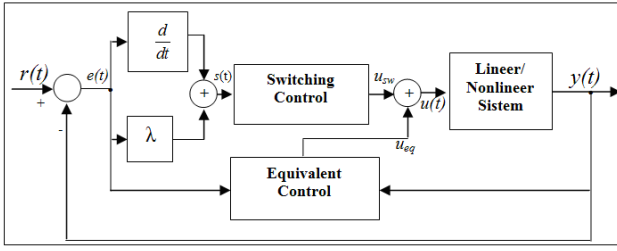
$$s = \dot{e} + \lambda e. \quad (8)$$

Fig. 5. Block diagram of sliding mode control.

When a sliding surface like in (8) is chosen, it can be written as the following equations:

$$\begin{cases} \dot{s} = \ddot{e} + \lambda \dot{e}, \\ e = x_{3ref} - x_3, \ \dot{e} = \dot{x}_{3ref} - \dot{x}, \ \ddot{e} = \ddot{x}_{3ref} - \ddot{x}_3, \\ x_{3ref} = \text{constant}, \ \dot{x}_{3ref} = \ddot{x}_{3ref} = 0, \end{cases} \quad (9)$$

$$\dot{s} = -\rho.sign(s) - K.s. \quad (10)$$

When a constant-proportional reachability rule like (10) is chosen, the following equations can be written.

$$\dot{s} = \ddot{e} + \lambda \dot{e} = \ddot{x}_{3ref} - \ddot{x}_3 + \lambda(\dot{x}_{3ref} - \dot{x}_3) =$$

$$= -\rho.sign(s) - K.s - \ddot{x}_3 + \lambda(-\dot{x}_3) =$$

$$= -\rho.sign(s) - K.s, \quad (11)$$

$$\ddot{x}_3 + \lambda \dot{x}_3 = \rho.sign(s) + K.s, \quad (12)$$

$$u = \frac{(-3.781x_3 \cos x_1 + 0.26432 x_3 \sin x_1 + 3.6775 x_3^2)}{x_3 + (3.781\cos x_1 - 0.26432\sin x_1 + \lambda).0.5 x_3^2} \times$$

$$\times (3.781\cos x_1 - 0.26432\sin x_1 + \lambda) +$$

$$+ \frac{0.25.(3.781\cos x_1 - 0.26432\sin x_1 + \lambda)}{x_3 + (3.781\cos x_1 - 0.26432\sin x_1 + \lambda).0.5 x_3^2} + \quad (13)$$

$$+ \frac{7.355 x_3 + \rho.sign(s) + K.s}{x_3 + (3.781\cos x_1 - 0.26432\sin x_1 + \lambda).0.5 x_3^2} =$$

$$= u_{eq} + u_{sw}.$$

VI. SIMULATION RESULTS

GASMC simulation results for WSCC systems have been obtained by using the Matlab/Simulink.

The phase space changing related to the power system with N-load-buses which was controlled by GASMC and SMC, has been given in Fig. 6. From the figure, the phase portrait related to the power system approaching to the origin is just like a spiral. The SMC error rate is higher than GASMC error rate. It shows that the system is asymptotically stable [16]–[18].

The Fourier coefficients which are obtained for GASMC methods are given in Fig. 7 and the frequency response is given in Fig. 8. The Fourier coefficients which are obtained by harmonics for tansig(.) has more pairs of complex conjugate poles along with in the s-plane. Left-half plane complex poles correspond to sinusoids multiplied by decaying exponentials, and right-half plane complex poles correspond to sinusoids multiplied by growing exponentials.
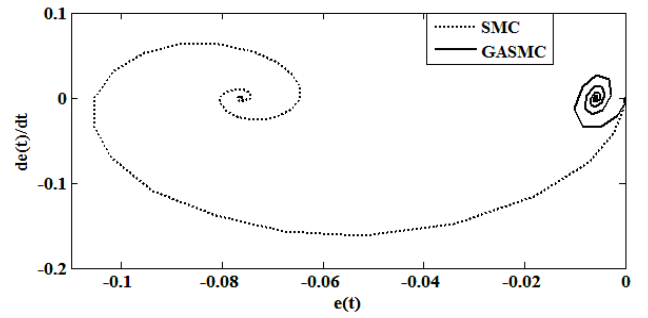

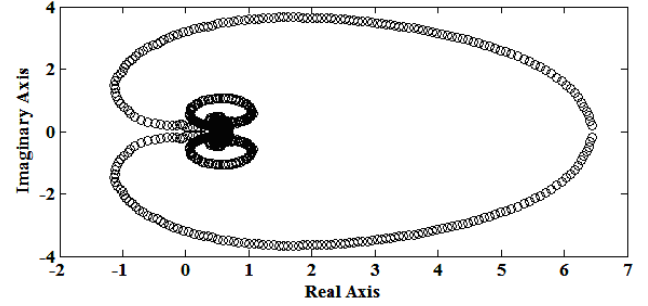Fig. 6. The phase plane of the SMC and GASMC systems.

Fig. 7. Fourier coefficients in complex plane for GASMC.

When the tansig(.) function is used in the structure of the GASMC and the amplitude of the signals is 40 to 0 in the GASMC method, the signal which has the effective frequency around 250 to 380 Hz which its noise harmonics are pressed, has been obtained in the Fig. 8.
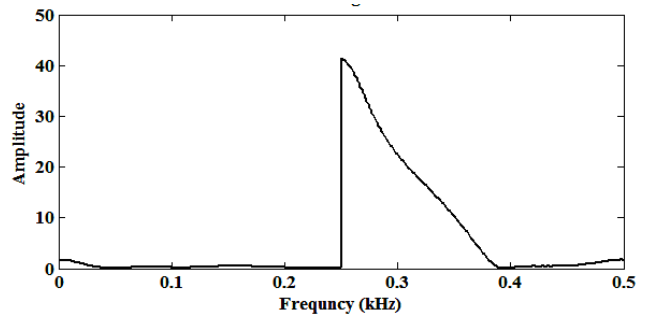

Fig. 8. Frequency domain display for GASMC control.

The unit step response curve related to N-load-bus power system with SMC and GASMC controller is given in Fig. 9. From the figure, with an appropriate steady state error, the V_2 output voltage reaches at the reference input in 5 seconds. The magnitude of the oscillation of SMC is rather high according to GASMC.
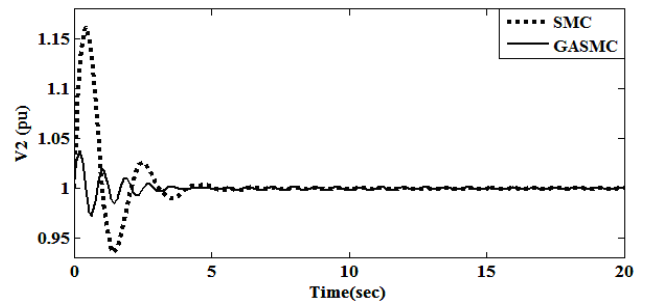

Fig. 9. The unit step response curves related to N-load-buses power system with SMC and GASMC controllers.
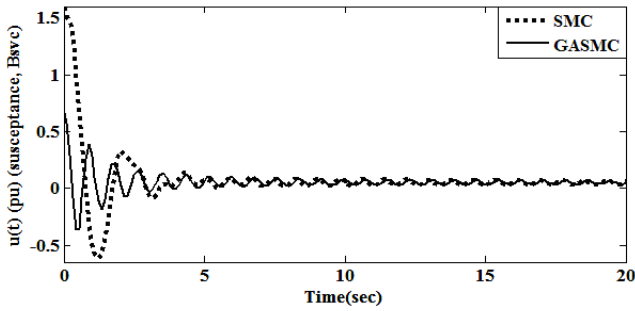
Fig. 10. The control signal $u(t)$ of the SMC and GASMC systems.

The control signal of the N-load-bus system with GASMC controller which is given in Fig. 10., starts with the amplitude of oscillation as ± 0.4, and approaching the equilibrium point by following a change which decreases the amplitude.
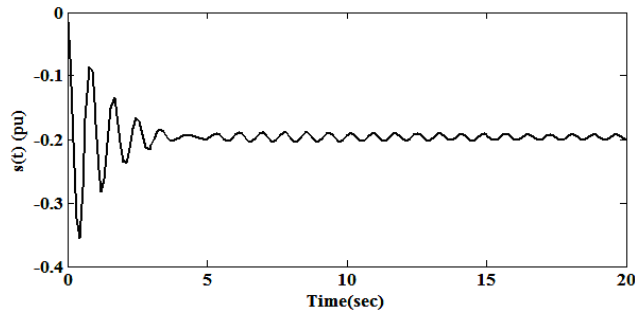

Fig. 11. Sliding surface $s(t)$ of the GASMC system.

The sliding surface of the N-load-bus power system with GASMC control, starts with an oscillation between the amplitude about -0.37 and -0.08 in the first seconds. After that, it is stabilized at the equilibrium point nearly at the 5th second and -0.2 pu.
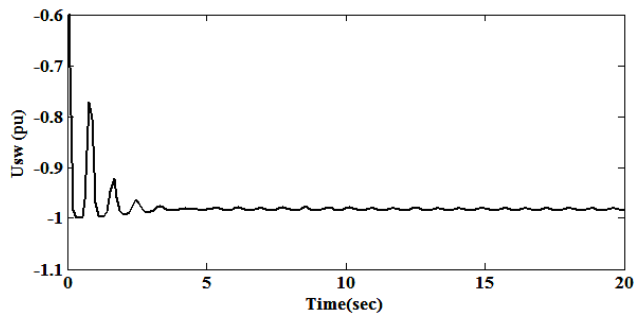

Fig. 12. The changing of the switching signal for GASMC system.

The switching input signal of the N-load-bus power system with GASMC controller, oscillates between the damping amplitude of -1 and -0.76 until the 5th second. And it shows that the signal stabilized between -0.99 and -0.98.

In Fig. 13, the load angle changes between in a bound of error tolerance about -4 degrees.

In the interval of the angular frequency change, the generator stays on synchronism on the angular velocity.

It is shown that the obtained results correspond to the data in the Table II for the power process of the power system [13].
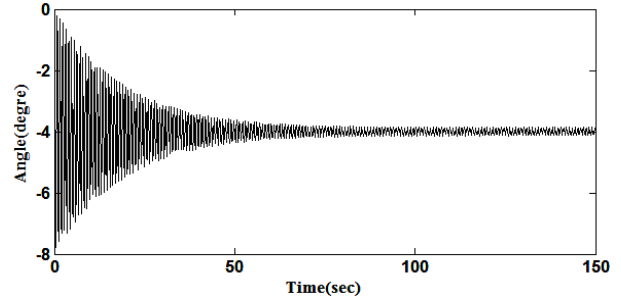

Fig. 13. The changing of the load angle related to N-load-bus power system with GASMC controller.
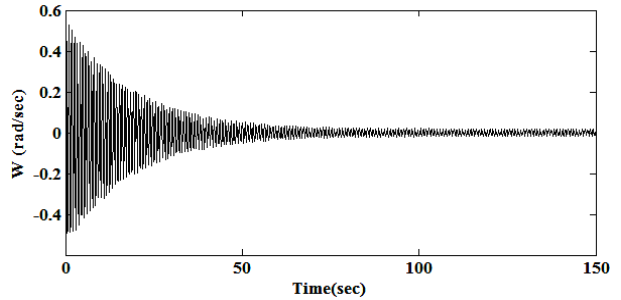

Fig. 14. The angular frequency change of the N-load-buses system according to time.

The control performance of the WSCC plant was significantly improved with the proposed GASMC which is better than the SMC controller.

VII. CONCLUSIONS

In this paper, WSCC three-machine nine-bus test systems with sliding mode control are proposed. From the power process results, number 5 load-bus has been chosen as the critical load-bus due to the fact that the voltage of the load-bus is less than 1 pu. The system is transformed to the system with two load-buses which are the reference load-bus and the number 5 load-bus after that the sliding mode mathematical model of this system has been obtained. The simulation results show that phase portraits related to power system reach at the origin as a spiral. The SMC error rate (-0.08) is higher than GASMC error rate (-0.01). This change shows the system is asymptotically stable. The Fourier coefficients in complex plane and frequency domain change support the spiral phase portrait. The angle and the angular frequency change correspond to Table II. The number-5 load bus angle given in Table II which is obtained by power flow and the number-5 load bus angle given in Fig. 13 which is obtained by simulation are compatible. The V_2 output voltage which is obtained for GASMC has low amplitude and permanent state error according to the results of SMC. The controller performance criteria of the V_2 output voltage were a maximum overshoot of % 15 for SMC and % 4 for GASMC, a setting time of 3 sec. for SMC and 5 sec. for GASMC and a steady state error of 2 sec. for SMC and 4 sec. for GASMC. GASMC has a far better response than SMC in improving the voltage for the number-5 bus in terms of the controller performance criteria.

REFERENCES

[1] A. Kurutia, T. Sakurai, "The power system failure", in *Proc. of 27th IEEE Conference on Decision and Control*, Austin, Texas, 1988, vol. 3, pp. 2093–2097.

[2] P. Acharjee, "Identification of Maximum Loadability Limit and Weak Buses Using Security Constraint Genetic Algorithm", *Electric Power and Energy Systems*, vol. 36, no. 1, pp. 40–50, 2012. [Online]. Available: http://dx.doi.org/10.1016/j.ijepes.2011.10.021

[3] C. Jaipradidthan, "Adaptive Neuro–fuzzy SVC for Multimachine Hybrid Power System Stability Improvement with Long of Double Circuit Transmission Lines", in *Proc. of the 2nd International Symposium On Neural Networks*, Chongqing, China, 2005, pp. 668–673.

[4] J. Wang, C. Fu, Y. Zhang, "SVC Control System Based on Instantaneous Reactive Power Theory and Fuzzy PID", *IEEE Transactions on Industrial Electronics*, vol. 55, no. 4, pp. 1658–1665, Apr. 2008. [Online]. Available: http://dx.doi.org/10.1109/TIE.2007.911933

[5] J. R. Smith, D. A. Pierre, I. Sadighi, M. H. Nehrir, J. F. Hauer, "A Supplementary Adaptive VAr Unit Controller for Power System Damping", *IEEE Transactions on Power Systems*, vol. 4, no. 3, pp. 1017–1023, Aug. 1989. [Online]. Available: http://dx.doi.org/10.1109/59.32593

[6] L. F. Li, K. P. Liu, M. Li, "Intelligent Control Strategy of SVC", in *Proc. of Transmission and Distribution Conference& Exhibition (PES 2005)*, Dalian, China, 2005, pp. 1–4.

[7] N. Karpagam, D. Devaraj, "Fuzzy Logic Control of Static Var Compensator for Power System Damping", *International Journal of Electrical and Electronics Eng.*, vol. 68, no. 2, pp. 625–631, 2004.

[8] R. Yan, Z. Y. Cong, T. K. Saha, J. Ma, "Nonlinear Robust Adaptive SVC Controller Design for Power Systems", in *Proc. of Power and Energy Society General Meeting – Conversion and Delivery of Electrical Energy in the 21st Cent.*, Pittsburgh, PA, 2008, pp. 1–7.

[9] F. F. Ewald, A. S. M. Mohammad, *Power Quality in Power Systems and Electrical Machines*. USA: Elsevier Academic Press, 2008 pp. 405–406.

[10] H. Wang, Z. M. Chen, J. G. Zhang, J. Meng, "Terminal Sliding Mode Control for Multi–Degree–of–Freedom Robot Based on Genetic Algorithm", in *Proc. of 5th International Conference on Natural Computation*, Tianjin, China, 2009, vol. 5, pp. 420–424.

[11] T. Wang, Q. Chi, C. Liu, "Parameter Identification and Compensation Control of Friction Model for PMSLS Based On Genetic Algorithms", in *Proc. of Chinese Control and Decision Conference*, Xuzhou, China, 2010, pp. 2391–2394.

[12] W. T. Huang, K. C. Yao, "New Network Sensitivity–Based Approach for Real–Time Complex Power Flow Calculation", in *Proc. of IET Generation, Transm. & Distrib*, Changhua, Taiwan, 2012, vol. 6, pp. 109–120.

[13] K. Abacı, "Bifurcation and Chaotic Analysis of The Line Conditioners for Voltage Stability" Ph.D. dissertation, Sakarya University, Institute of Science, Sakarya, Turkey, 2007, p. 148.

[14] I. P. Reddy, "Control strategy and Placement of FACTS Devices for damping of Power System Osillations", Ph.D. dissertation, Jawaharlal Nehru Technological University, Hyderabad, India, Jul. 2011.

[15] R. Hooshmand, M. Ataei, A. Zargari, "A New Fuzzy Sliding Mode Controller for Load Frequency Control of Large Hydropower Plant Using Particle Swarm Optimization Algorithm and Kalman Estimator" *European Transactions on Electrical Power*, 2011. [Online]. Available: http://dx.doi.org/10.1002/etep.609

[16] M. Ahmed, "Sliding Mode Control for Switched Mode Power Supplies", Ph.D. dissertation, Lappeenranta University of Technology, Digipaino, Lappeenranta, Finland, 2004. p. 97.

[17] İ. Eker, "Sliding Mode Control with PID Sliding Surface and Experimental Application To An Electromechanical Plant", *ISA Transactions*, vol. 45, no. 1, pp. 109–118, Jan. 2006. [Online]. Available: http://dx.doi.org/10.1016/S0019-0578(07)60070-6

[18] İ. Eker, "Second Order Sliding Mode Control with Experimental Application," *ISA Transactions*, vol. 49, no. 3, pp. 394–405, Jul. 2010. [Online]. Available: http://dx.doi.org/10.1016/j.isatra.2010.03.010